IOP PUBLISHING JOURNAL OF PHYSICS D: APPLIED PHYSICS

J. Phys. D: Appl. Phys. **41** (2008) 055306 (4pp) doi:10.1088/0022-3727/41/5/055306

Enhanced surface diffusion in forming ion-beam-induced nanopatterns on Si (0 0 1)

R Banerjee, S Hazra and M K Sanyal

Surface Physics Division, Saha Institute of Nuclear Physics, 1/AF Bidhannagar, Kolkata 700 064, India

E-mail: milank.sanyal@saha.ac.in

Received 4 January 2008
Published 14 February 2008
Online at stacks.iop.org/JPhysD/41/055306

Abstract

The diffusion process on Si (0 0 1) in the presence of a 5 keV Ar^+ ion beam has been investigated by monitoring initiation of ripple-pattern formation. The morphology of the surface obtained by scanning tunnelling microscopy measurements in ultrahigh vacuum were characterized using the height-difference correlation function. These measurements clearly show formation of nanostructured ripple patterns having wavelength ~60 nm and height ~0.32 nm at 200 °C. The results demonstrate that ion beam induced and thermal diffusions cannot be treated as additive processes and the observed enhancement of surface diffusion requires lowering of activation energy that arises due to creation of ion-beam induced vacant regions.

(Some figures in this article are in colour only in the electronic version)

1. Introduction

The understanding of diffusion process on silicon surface is of fundamental importance [1] for the development of nanoelectronic devices. The diffusion process becomes enigmatic when ion beam and temperature are used simultaneously [2]. Better understanding of this subject is required as focused ion-beams are increasingly being used in the fabrication of nanodevices [3]. The formation of ripple-like patterns in nanometre scale, on silicon surface with obliquely incident ion beam, similar to that observed in metre scale in sand dunes of the deserts [4–11], provides a method to investigate diffusion processes [6]. Statistical models have been developed [5] to explain the morphological features of the ion-beam induced ripple patterns that arise due to the balance between erosion and diffusion processes. These models have successfully predicted wavelength of the generated ripples, given as $\lambda = 2\pi\sqrt{2K_{\text{eff}}/|\nu|}$ with K_{eff} as effective surface diffusion constant and ν as the effective surface tension associated with the erosion process [5]. It is generally assumed that effective surface diffusion is a simple superposition of independent thermal and ion-beam induced contribution as $K_{\text{eff}} = K_{\text{thermal}} + K_{\text{ion}}$ [5, 6]. It is known that K_{thermal} exhibits conventional Arrhenius behaviour [5, 12] $K_{\text{thermal}} = (K_0/T)\exp(-E_a/k_BT)$ and K_{ion} is independent of temperature (T). Systematic surface diffusion studies [13, 14] have shown that the presence of a low energy ion beam can modify both the activation energy E_a and the pre-exponential factor K_0 of the thermal diffusion constant. It was observed in a study [2] of ripple-pattern formation on a Si (0 0 1) surface with 750 eV Ar^+ ion beam that the value of E_a is about 1.2 eV at 550 °C, which is much less than the expected value of about 2 eV [1]. We have investigated, with a ultrahigh vacuum (UHV) scanning tunnelling microscope (STM) set-up, the initiation of ripple-pattern formation on Si (0 0 1) at lower sample temperatures using a 5 keV Ar^+ ion beam and have found clear signature of ripple formation even at 200 °C.

2. Experimental

The Si (0 0 1) sample, typically $1 \times 1\ \text{cm}^2$, glued to a stainless steel sample plate using silver adhesive was transferred to an UHV (10^{-9} mbar) analysis chamber (Omicron) for surface modification and to study morphology. The cleaning and modifications of the surface were carried out using a 5 keV cold cathode Ar^+ ion source (ISE 5, Omicron) by placing the sample on a manipulator. The imaging of the top surface was carried out in constant current mode using a STM (Omicron), attached

 © 2008 IOP Publishing Ltd Printed in the UK

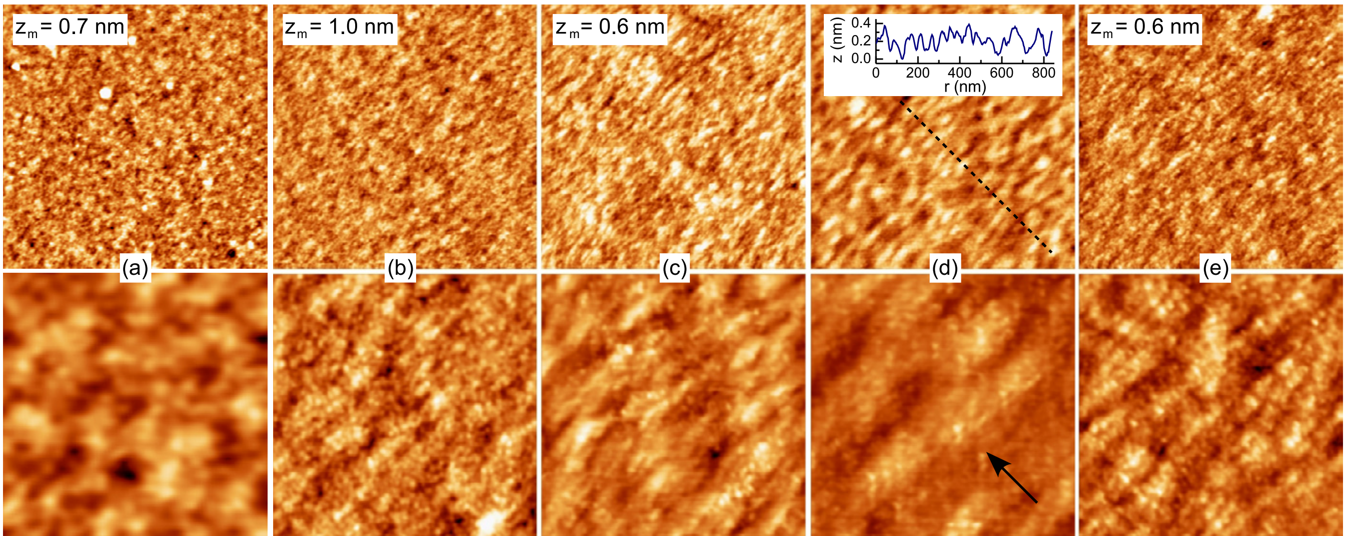

Figure 1. STM images of (*a*) oxide removed unmodified Si surface and (*b*)–(*e*) low energy ion-beam modified Si surface at four different stages of modification (as mentioned sequentially in table 1), in two magnifications. Top panel for scan size 1000 × 1000 nm^2, while lower panel for scan size 200 × 200 nm^2. z_m indicates the height corresponding to the maximum variation in the colour code, the arrow indicates the ion-beam direction and the inset of (*d*) shows typical line profile.

to the same analysis chamber. For the removal of the oxide layer from the top of the Si sample, 0° incident angle of the ion beam with respect to the surface normal was used, while for the surface modifications that angle was kept at 60°. However, due to the position of the ion source in the chamber, some constant azimuthal angle (about 37°) was unavoidable. The operating pressure and the beam current during the sputtering experiment were about 2.5×10^{-5} mbar and 20 μA, respectively. The sample was kept at a fixed temperature using resistive heating arrangement at the manipulator stage and was monitored using a K-type chromel–alumel thermocouple. In figure 1(*a*) we have shown a STM image of the Si (0 0 1) surface after the removal of the oxide layer with ion-beam irradiation. We investigated ripple-pattern formation by studying surface morphology of the Si (0 0 1) surface after exposing it to a 5 keV ion beam as a function of temperature. We could not detect any signature of ripple-pattern formation until we kept the sample temperature at 200 °C. Representative STM images of the modified Si (0 0 1) surface kept at 200 °C are shown in figures 1(*b*)–(*e*) that clearly indicate the initiation of ripple-pattern formation. Figures 1(*b*) and (*c*) represent surface conditions after 15 min and 30 min of ion-beam irradiation, respectively, keeping the sample temperature at 200 °C. We then kept the sample at this temperature and switched off the ion beam (refer figure 1(*d*)) for 30 min and finally switched on the ion beam again for another 30 min (figure 1(*e*)) at 200 °C. In table 1 we have shown wavelength of ripple-patterns and other associated morphological features obtained from the STM images of the sample at various stages.

3. Results and discussion

Domains start growing in one direction from the stage S15–S30 (refer figures 1(*b*) and (*c*)) and a clear signature of ripple-pattern formation is obtained for S30A (refer figure 1(*d*)). The direction of growth is perpendicular to that of the ion beam, as observed in the ion-induced patterns. However, further bombardment in the presence of temperature for S30A30 (see figure 1(*e*)) makes the surface irregular, although height fluctuation is still very small. We believe this indicates transition from the linear to the nonlinear regime that is typically accompanied by the disappearance of ripples and the appearance of rotated ripple structure [5, 15]. In our data rotation of ripples is not clear and we also do not observe any increase in ripple amplitude (refer table 1). We obtain the average wavelength (λ) and the amplitude (A) estimated from the STM images (refer table 1) by drawing line profiles along the ion-beam direction and approximating the ripple-like patterns with a simple form $A\cos(2\pi r/\lambda)$. Ripple patterns having an amplitude of 0.32 nm and a large wavelength (λ) of 60 nm could be observed due to the UHV condition of the chamber.

Table 1. Parameters (A is the amplitude of the ripples, λ is the ripple wavelength, $\xi_\parallel$ is the correlation length parallel to the ion beam direction, $\xi_\perp$ is the correlation length perpendicular to the ion beam direction, $\alpha_\parallel$ is the scaling exponent parallel to the ion beam direction, $\alpha_\perp$ is the scaling exponent perpendicular to the ion beam direction) for the ion-beam modified Si surface at different stage of modification obtained from the analysis of STM images. The four different stages are S15 (sputtering for 15 min), S30 (sputtering for 15 + 15 min), S30A (sputtering for 15 + 15 min followed by switching off the ion-beam for 30 min), S30A30 (sputtering for 15 + 15 min followed by switching off the ion-beam for 30 min and then sputtering for 30 min). All experiments were carried out at 200 °C.

Label	A (nm)	λ (nm)	$\xi_\parallel$ (nm)	$\xi_\perp$ (nm)	$\alpha_\parallel$	$\alpha_\perp$
S15	0.36	70	12	19	0.90	0.85
S30	0.32	58	11	22	0.90	0.85
S30A	0.32	60	18	40	0.91	0.83
S30A30	0.32	60	10	19	0.90	0.75

For analysing the observed initiation of ripple structure, we used the height-difference correlation function of the

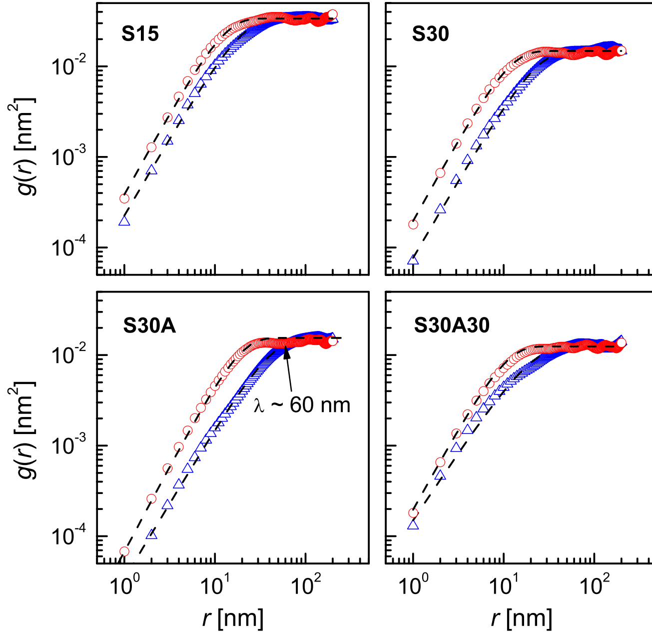

Figure 2. Height-difference correlation function of low energy ion-beam modified Si surface at four different stages of modification, parallel (○) and perpendicular (Δ) to the ion-beam direction. The symbols represent the data estimated from STM images, while the dashed lines are the fit corresponding to equation (2).

following form [16–18]:

$$g(r) = \langle (h(r_0 + r) - h(r_0))^2 \rangle, \qquad (1)$$

where $h(r_0+r)$ is the height of the surface at a relative position r and $h(r_0)$ is the mean surface height. Equation (1) has been used to calculate statistically meaningful $g(r)$ from the STM images. An average of the correlation function obtained from two different scan lengths for the same area along the two perpendicular directions for the surface at four different stages is shown in figure 2. A nearly linear increase up to a certain length scale followed by saturation is observed in all the curves. The length scale, where the saturation is observed, is found to be smaller along the ion-beam direction for all stages of the modified surface.

It is known that the height-difference correlation function, for many rough surfaces can be approximated as [19, 20]

$$g(r) = 2\sigma_0^2[1 - \mathrm{e}^{-(r/\xi)^{2\alpha}}], \qquad (2)$$

where σ_0 is the saturation roughness, ξ is the correlation length and α is the scaling exponent of the surface. The height-difference correlation data of the different modified surface stages have been fitted using equation (2), and the fits are presented in figure 2. The associated parameters obtained from the analysis are listed in table 1. It can be noted from the table that the value of the scaling exponent, parallel ($\|$) to the ion-beam direction is more than that in the perpendicular ($\perp$) direction; however, the situation is reverse for the value of the correlation length. $\xi_\perp > \xi_\|$ suggests that ion bombardment produces more diffusion in the perpendicular direction compared with the parallel one. With the dose, $\xi_\perp$ increases and is particularly prominent for the post annealed surface. However, for further bombardment, the value of the perpendicular correlation length ($\xi_\perp$) decreases for the post-anneal bombardment (figure 1(*e*)) and is almost comparable to the perpendicular correlation length ($\xi_\perp$) for pre-anneal bombardment (figure 1(*c*)). This again suggests transition from the linear to the nonlinear regime.

4. Conclusion

In summary, we have observed initiation of ripple-pattern formation with a 5 keV Ar^+ ion-beam on the Si (0 0 1) surface provided the sample temperature is maintained over 200 °C. The wavelength and amplitude of the ripples remain almost constant at around 60 nm and 0.32 nm, respectively. The value of the effective surface diffusion constant $K_{\mathrm{eff}} (= \lambda^2|\nu|/8\pi^2)$ turns out to be 5.1 $\mathrm{nm^4\,s^{-1}}$ with $\nu = -0.11\ \mathrm{nm^2\,s^{-1}}$ as calculated following the standard expressions [5]. The value of K_{thermal} calculated from the Arrhenius equation with even the value of E_a as 1.2 eV as obtained earlier [2] is found to be $2 \times 10^{-4}\ \mathrm{nm^4\,s^{-1}}$—four orders of magnitude less than K_{eff}. Hence one can assume that thermal diffusion is negligible here and ion-induced diffusion K_{ion}, which scales with $|\nu|$ for fixed energy and angle of incidence [5], is the dominating term and is expected to determine K_{eff} as $K_{\mathrm{eff}} = K_{\mathrm{thermal}} + K_{\mathrm{ion}}$. But the requirement of 200 °C sample temperature and difference of patterns between S30 and S30A (refer figure 2 and table 1), even when the ion beam is switched off, clearly indicate that thermal diffusion is important here and cannot be treated as an additive term. To ensure that K_{thermal} becomes comparable to K_{eff}, one has to either put a large (10^4) pre-factor or reduce the E_a to around 0.8 eV. Systematic reduction of E_a has been experimentally observed earlier for Ar^+ ion energy for more than 15 eV [14]. The reduction of E_a was also observed in a STM study of the Si (1 1 1) surface and it was found that E_a remains low even when [21] the ion beam is turned off after the creation of vacant regions. It has been predicted [22] theoretically that E_a can take a low value like 0.8 eV due to vacancy mediated diffusion. A large periodicity (60 nm) of ripple pattern with amplitude (0.32 nm) less than the lattice parameter observed here also indicates vacancy mediated diffusion. It seems ion beam induced vacancies lower the effective activation energy of thermal diffusion and hence ion induced diffusion and thermal diffusion processes cannot be considered as two independent additive terms in determining the effective diffusion constant K_{eff}. Further studies are required to make nanoscale ripple structures a viable route for device fabrication process and to understand the interplay between thermal and ion-induced terms in the surface diffusion process.

Acknowledgment

The authors are grateful to Professor T K Chini for valuable discussions.

References

[1] Caliste D and Pochet P 2006 *Phys. Rev. Lett.* **97** 135901
[2] Erlebacher J, Aziz M J, Chason E, Sinclair M B and Floro J A 1999 *Phys. Rev. Lett.* **82** 2330
[3] Kitslaar P, Strassner M, Sagnes I, Bourhis E, Lafosse X, Ulysse C, David C, Jede R, Bruchhaus L and Gierak J 2006 *Microelectron. Eng.* **83** 811
[4] Mayer T M, Chason E and Howard A J 1994 *J. Appl. Phys.* **76** 1633
[5] Makeev M A, Cuerno R and Barabasi A-L 2002 *Nucl. Instrum. Methods* B **197** 185
[6] Chini T K, Sanyal M K and Bhattacharyya S R 2002 *Phys. Rev.* B **66** 153404
[7] Hazra S, Chini T K, Sanyal M K, Grenzer J and Pietsch U 2004 *Phys. Rev.* B **70** R121307
[8] Valbusa U, Boragno C and de Mongeot F B 2002 *J. Phys.: Condens. Matter* **14** 8153
[9] Carter G 2001 *J. Phys. D: Appl. Phys.* **34** R1
[10] Kim J, Cahill D G and Averback R S 2003 *Phys. Rev.* B **67** 045404
[11] Grigorian S, Pietsch U, Grenzer J, Datta D P, Chini T K, Hazra S and Sanyal M K 2006 *Appl. Phys. Lett.* **89** 231915
[12] Brown A-D and Erlebacher J 2005 *Phys. Rev.* B **72** 075350
[13] Ditchfield R and Seebauer E G 1999 *Phys. Rev. Lett.* **82** 1185
[14] Ditchfield R and Seebauer E G 2001 *Phys. Rev.* B **63** 125317
[15] Datta D P and Chini T K 2004 *Phys. Rev.* B **69** 235313
[16] Barabási A-L and Stanley H E 1995 *Fractal Concepts in Surface Growth* (Cambridge: Cambridge University Press)
[17] Yang H-N, Zhao Y-P, Chan A, Lu T-M and Wang G-C 1997 *Phys. Rev.* B **56** 4224
[18] Basu J K, Hazra S and Sanyal M K 1999 *Phys. Rev. Lett.* **82** 4675
[19] Sinha S K, Sirota E B, Garoff S and Stanley H B 1988 *Phys. Rev.* B **38** 2297
[20] Fenner D B 2004 *J. Appl. Phys.* **95** 5408
[21] Yoneyama K and Ogawa K 1996 *Japan. J. Appl. Phys.* **35** 3719
[22] Pankratov O, Huang H, Diaz de la Rubia T and Mailhiot C 1997 *Phys. Rev.* B **56** 13172